Engineering and Technology Journal
Journal homepage: https://etj.uotechnology.edu.iq

Optimization of Design Parameters for Manufacturing a Radial Active Magnetic Bearing with 12-Poles

Mohamed N. Hamad *, Muhannad Z. Khalifa, Jamal A. K. Mohammed

Electromechanical Engineering Dept., University of Technology, Baghdad-Iraq, Alsina'a street, 10066 Baghdad, Iraq.
*Corresponding author Email: jawadimohamed79@gmail.com

HIGHLIGHTS

- Designing a radial Active Magnetic Bearing (AMB) after performing an optimization process via reducing the number of poles.
- Reduction of the complexities of the control system is inversely proportional to the number of poles.
- It was noticed that increasing the rotational speed would increase the torque.
- The model covered in this study is made of a material with good engineering and magnetic characteristics steel 37-2.

ARTICLE INFO

Handling editor: Muhsin J. Jweeg
Keywords:
Active magnetic bearing; Air gap
Optimal design; ANSYS Maxwell

ABSTRACT

This research aims to design an Active Magnetic Bearing (AMB) after performing an optimization process via reducing the number of poles and by reducing air gap, Dia. Yoke, and Z-length (deep of model). To increase the performance of a radial Active Magnetic Bearing (AMB), all particular equations of design based on the Genetic Algorithm method by using ANSYS Maxwell (Version 17.1) program of electro-magnetic have been studied. Manufacturing an active magnetic bearing standing for two counts, each one containing 12 poles instead of 16, led to a significant improvement in the performance. Some conclusions were obtained, including the complications in the control system will be reduced when they are linked in AMB. The complexities of the control system are inversely proportional to the number of poles and the model covered in this study is made of a material with good engineering and magnetic characteristics steel 37-2.

1. Introduction

Active Magnetic Bearings (AMBs) are used mainly in high-speed machinery due to their contactless operation. The large size of the AMB is one of its main drawbacks. It may be thought of in Compact AMBs with a higher load-carrying capacity to better use of space and material available. In light of this, an attempt was made by Rao and Kakoty [1] for designing compact AMBs to get higher load-carrying capacity. Two main parameters are considered, namely the leg shape and the pattern of the pole winding. The effect of these parameters on the load-carrying capacity as well as the AMB size has been evaluated. Yeh [2] proposed a semi-AMB system that includes both the passive and active magnetic bearings for rotatory machine applications. In particular, the issues of the design, the analysis, and the control of the semi-active system were investigated using an axial fan as the platform. In the proposed system, while the rotor is axially lifted by the active bearing, its tilting and radial stability are ensured by the passive bearings. Martynenko [3] had found a way to reduce the vibration amplitudes of turbo-machinery rotors with passive and active magnetic bearings in resonances and resonance areas corresponding to one of the critical speeds ranging from zero to those operating rotations. The method is based on the ability to change the nonlinear strength and the damping properties of the novel design of the PMBs and AMBs via varying the electrical parameters of electromagnet circuits. They confirmed the possibility of using passive/active magnetic suspensions for rotors having lightweights (e.g., compressors and expanders) with the achievement of the proposed method of detuning from resonance situations. Anshan et al. [4] studied a rotor that serves as a rotating structure driven by a 4KW AC motor through couplings and suspended by an active magnetic bearing with its position Sensors and Hall Effect Sensors connected in place connected to the main computer. A digital link that interfaces between the DSP and the general mathematics program are made to run on the computer in which all the forces and the displacement signals are available in analog which then processed and finally display the results. Modal analysis was then performed for the free-free boundary conditions for the rotor system with bearing

http://doi.org/10.30684/etj.v40i1.2202
Received 01 June 2021; Accepted 22 August 2021; Available online 25 January 2022
2412-0758/University of Technology-Iraq, Baghdad, Iraq

conditions when the rotor speed was equal to 20000rpm. Attica Hila et al. [5] showed the influence of dynamic characteristics of an AMB on the dynamic response and stability of an unbalanced and asymmetric rotor. Indeed, the AMBs have been successfully employed in many industrial machinery facilities. Their main advantages are the principle of non-contact work, operating at very high speeds, and suspension without friction. At first, through electromagnetic theory, the AMBs dynamic supporting parameters were obtained. After that, the generalized system motion equations were derived using the finite element method (FEM). Spece et al. [6] studied the axial magnetic bearing actuators and determined the dynamic performance of the axial magnetic suspension as they lead to a much lower bandwidth of actuator (f < 50 Hz) than that bandwidth enjoyed by a radial AMB (f >1000 Hz). Due to the importance of eddy currents to the thrust dynamic performance of an AMB, great efforts were made for developing useful analytical models that predict the frequency response of an actuator from material properties and geometry. This possibility is exploited here, to show the improvements which may be obtained and to clarify the relationship between different parameters and the dynamic performance. Ran et al. [7] presented a modeling frame and detailed design for high-speed flexible rotor supported by AMBs and an effective framework of synthesizing powerful controllers for high-speed flexible rotor exposed to resonant vibration by using mixed-sensitivity H∞ control. It has shown that modal testing effectively contributes to the accuracy of the rotor model, which is very important for robust model-based control. By double fine-tuning the uncertainty weighting functions, an H∞ mixed-sensitivity controller was designed. Zairian et al. [8] studied that one of the major problems which are faced by a magnetic bearing rotor system is the rotor crack fault. To enhance the safety performance of this type of machinery, it is necessary for studying the characteristics of the vibration of the magnetic bearing system with the cracked rotor. In this study, the hardness model of the cracked shaft element was established by the theory of Strain Energy Release Rate (SERR). The main objective of this research is to manufacture active magnetic bearing with every detail. Before manufacturing, a model consisting of 16 poles with dimensions and metal was chosen, the theoretical optimization design was performed, and then the manufacturing was done.

2. Working principle of amp

The magnetic bearing is shown in Figure 1 works on the electromagnetic suspension principle depending on inducing eddy currents in a moving conductor. When a conductor is moving in a magnetic field, a current will be produced in the conductor. This current will oppose the magnetic field changes according to Linz's law. This will generate a current producing a magnetic field in opposite direction to that of the magnet. Thus the electrically conductive material acts as a magnetic mirror [9]. The AMBs are used to raise the rotating shaft across electromagnetic forces. The bearing rotor at the central line is organized by closed-loop feedback via position sensors, power amplifiers, a digital controller, and electromagnets as shown in Figure 2. The bearing system also contains an external power supply and auxiliary mechanical magnetic bearings for supporting the rotor shaft in case of AMB failure occurrence [9].

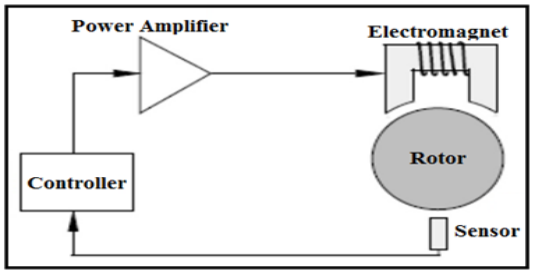

Figure 1: Basic principle of an AMB [9]

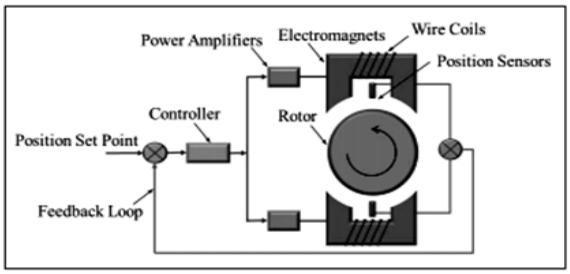

Figure 2: Basic active magnetic bearing components [9]

3. Optimal design method for the amp: theory

In the present paper, ANSYS Maxwell software version 17.1 is used to analyze a single-axis double-winding AMB in a 2-D and a 3-D model. The ANSYS Maxwell has several FEA features ranging from complex to linear, dynamic, transient, etc. Calculating the flux pattern, field strength, and force using ANSYS Maxwell is shown via the flowchart of Figure 3. The calculation of flux, field strength, and force of the AMB is depending on Maxwell's electromagnetism equations. Maxwell's equations can be written in the differential form as [10, 11].

$$\nabla B = 0 \tag{1}$$

$$\nabla D = \rho \tag{2}$$

$$\nabla \times E = -\frac{\partial B}{\partial t} \tag{3}$$

$$\nabla \times H = J + \frac{\partial D}{\partial t} \tag{4}$$

For static magnetic field:

$$\frac{\partial D}{\partial t} = 0, \quad \text{so} \quad \nabla \times H = J \tag{5}$$

$$B = \mu H = H\mu_o\mu_r \tag{6}$$

$$D = \varepsilon E = \varepsilon_o\varepsilon_r E \tag{7}$$

$$J = \sigma E \tag{8}$$

$$F = Q(E + \nabla \times B) \tag{9}$$

Before starting to manufacture the magnetic bearing, it should be optimized by using the Analyse Maxwell program specializing in electromagnetism. Figure 3 shows the flowchart of optimal design for the active magnetic bearing [11], where the boundary conditions are indicated in the following steps below:

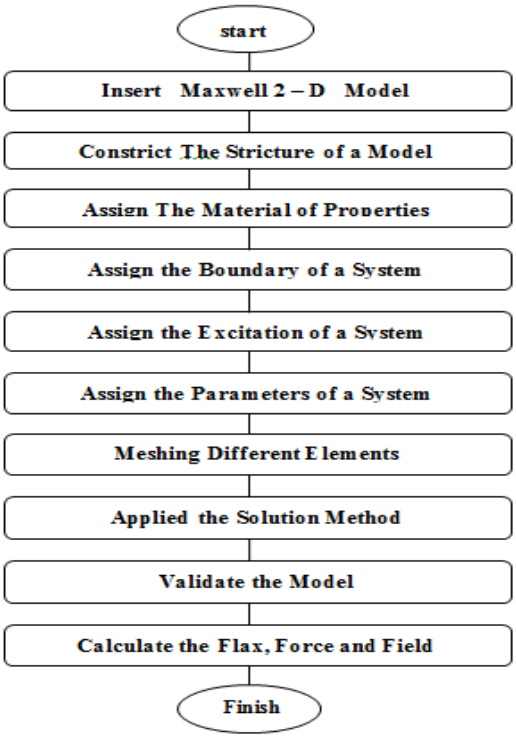

Figure 3: Flow Chart of Optimal Design for the AMB [11]

As the program is finished shown in Figures 4 and 5, an active magnetic bearings (AMBs) controller with a flexible rotor system has been designed. Depending on the FEM, the movement equations of the AMBs and flexible rotor system were built. The weighting function matrices of the H∞ controller have been studied for both the sensitivity and complementary sensitivity according to the H∞ control theory. Experiments were carried out on 4-degree freedom magnetic bearings with a flexible rotor test rig. The experimental results proved that the method of H∞ control has a better ability to lower the vibration than conventional PID control. The H∞ controller has effective interference immunity and strong stability. The peak to peak amplitudes of vibration for the flexible rotor is less than 60μm at the first critical flexible rotor speed. The findings show that the H∞ controller for the AMBs with a flexible rotor system is stable through the first critical speed of the flexible rotor system [12].

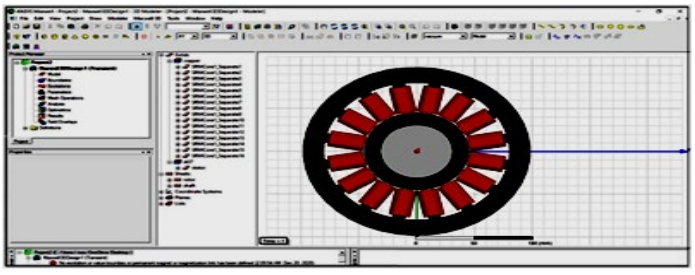

Figure 4: Model before design process optimization of active magnetic Bearing with 16 poles drawn by ANSYS Maxwell (Version 17.1)

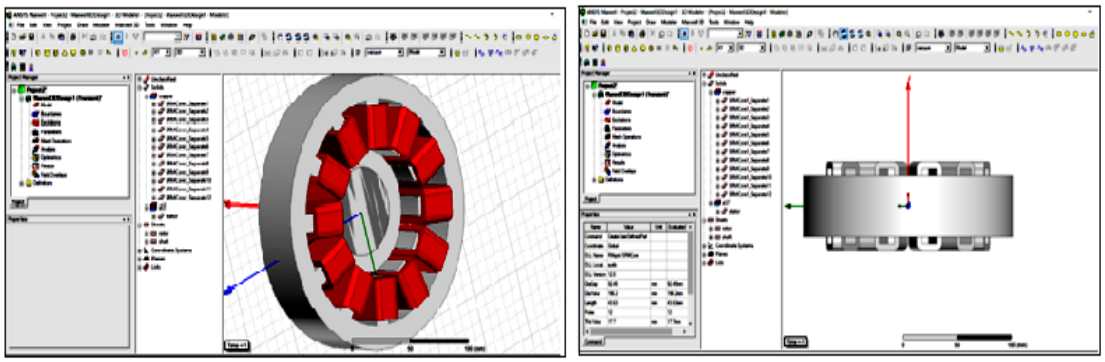

Figure 5: The side and top view for active magnetic bearing with 12 Poles

4. Manufacturing steps of the proposed radial amp

The radial AMB was manufactured according to its design equations depending on the optimal design by genetic algorithmic method, in addition, according to materials used in the manufacture of the magnetic stand, as described in the following steps:

4.1 Choose the type of metal used

The metal was chosen in manufacturing the proposed radial AMB is steel 37-2. This metal has high-performance features, as well as, it is considered one of the Ferromagnetic materials with high magnetism. Table 1 shows the Chemical composition for ST 37-2 at temperature 25 ^{o}C and humanity 49% with all properties shown in Table 2. Moreover, it is considered a low carbon mineral, as it gives good results in the performance efficiency of the magnetic bearing. All examination results for this metal were carried out in the company for engineering examination and rehabilitation.

Table 1: Chemical Composition for st37-2 used in AMB

Steel Grade	C %	Si %	M%	P %	S %	Ni %	Al %	Cu %	Mo %	Fe%
ST37-2	0.123	0.237	0.722	0.0115	0.0072	0.0242	0.389	0.0056	0.0034	Bal

Table 2: The Properties of st37-2 used in AMB

Properties	Values
Conductivity at 25 ^{o}C	30 MS/m
Ultimate stress	385- 400 N/mm^2
Hardness Test (HRB)	70

4.2 The Number of Poles for AMB after Optimization Design

The choice of the number of poles is very necessary, especially in the design and manufacture of the magnetic bearing. To keep away from the complex design and to obtain easy control of its work and efficiency, the 16-poles were initially selected. After optimizing the design to improve the performance, the number of poles became 12 poles as shown in Figure 6. Table3 shows all dimensions.

(a) AMB Basic Structure of with Pole Numbering (b) Two AMBs with Same Dimensions

Figure 6: Manufactured Structures of the AMB

Table 3: Specifications of the Manufactured AMB

No.	Parameters Name	Values After Optimal
1	Number of Poles	12
2	Dia. Gap or inner dia. of stator	92.30 mm
3	Dia. Yok or (outer Dia. of stator)	188.92 mm
4	Length or Depth (Stator Axial Length)	39.267 mm
5	ThkYoke (Thickness of Yok)	14.16 mm
6	Leg Dimension (Stator Leg Dimensions)	10*34.15 mm
7	Stator weight (Mass) Material of Stator	4.922 kg ,48.3 N Steel grade 37, Density = 7.81 kg/m^3 & Elastic modulus =201GN/m^2
8	Nominal Air Gap	0.85 mm
9	Rotor Lamination Outer Diameter	90.4 mm
10	Copper Turns Per Stator Leg	3000 turn
11	Embrace (the ratio of pole arc to pole pitch)	0.411 mm
12	Wire Gauge, Diameter, and Cross Section Area	# 35 AWG, D=0.01 mm & A = $0.785*10^{-4}$ mm^2
13	Mass winding for one coil	60 g
14	Connections	Three phases
15	Maximum Current (I_{max})	1.8 A
16	Winding Temperature (T_i)	10°C

Figure 7 shows the mass of one pole after optimal design; while Figure 8a shows that the gauge length for the normal distance between every two opposite poles is about 95.86 m. Figure 6b shows that the gauge of stator width is about 40.22 mm.

Figure 7: The Mass of One Pole

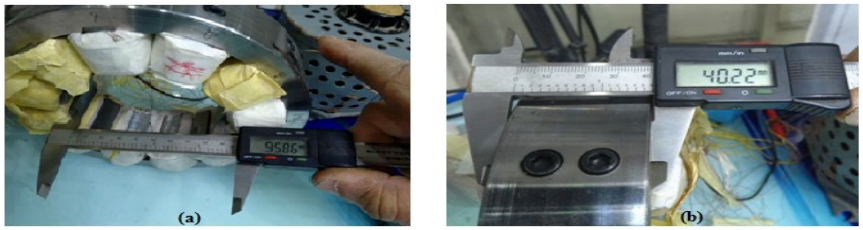

Figure 8: (a) Dimension of Normal Distance Between Each Two Opposite Poles and (b) Gauge of Stator Width

4.3 Method of winding with respect to the pole

The winding method determined concerning the coil is called the heteropolymer method of the radial bearings and it is the most common method in magnetic bearings due to its simplicity, cost-effectiveness, and performance. These properties increase the performance efficiency of the radial AMB. Figure 9 shows (a) the process of wrapping the windings around four poles to provide the first phase, (b) wrapping all poles, and (c) the insulation process of the windings of the poles as well as the poles fixed screws. Copper wire with gauge # 35AWG was chosen to build the coils with 3000 turns each. The copper material is preferred as the best conductive material for windings, as it has very high conductivity, which leads to decrease the power losses and high temperature and thus reduce the eddy currents to less as possible this will therefore will lead to an increase in the amount of magnetic flux generated in the coils. Figure 10 shows the value of measuring the weight mass of copper coil block to one pole with about 70.18 g.

Figure 9: Steps of wrapping the poles

Figure 10: the mass of the copper coil block for one pole

4.4 Power supply of the manufactured AMB

The radial AMB has been fed by an AC three-phase supply to obtain high stability of the bearing operation, in addition, to getting a stronger magnetic force than other AMB types thus enhancing the performance of the magnetic bearing.

4.5 The control system to the AMB

The moving part can be regulated in the midline by closed-loop feedback control utilizing position sensors, digital control unit, electromagnets, and power amplifiers to ensure that the rotor movement is controlled and remains out of contact with the ends of the electrodes and the magnetic force is generated so that the rotor remains fixed on the center line. Figure 11 shows the photoelectric sensor type PNP laser for reading the displacement in the X and Y axes. Figure 12 shows the small control of the AMB.

5. Manufactured system components

Depending on the ANSYS Maxwell program (version 17.1) for electromagnet, the optimal design of the ABM was carried out. So, on this basis the system was built as follows:

5.1 Rotor

His rotor shown in Figure 13 is made of metal type steel 37-2 with 12.197 kg; its mass was measured in Engineering Testing and Qualification Company of the Ministry of Industry and dimensions of the total length 68 cm, the outer diameter of 60 mm, an inner diameter of 36 mm.

5.2 The AMB

Figure 14 shows the front and rear sides of the two AMBs for supporting the rotor.

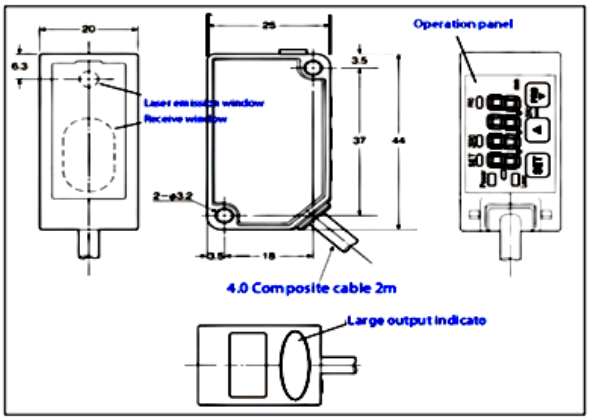

Figure 11: PNP laser sensor

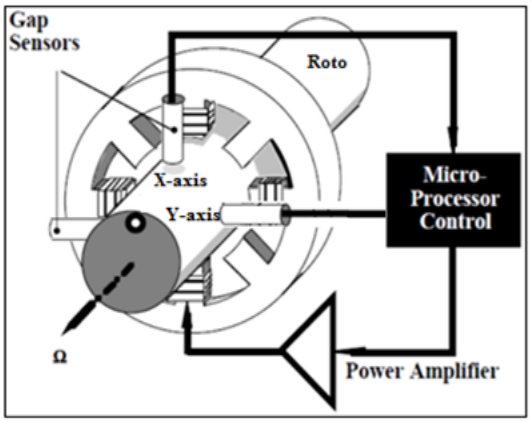

Figure 12: Small control circuit of the AMB

Figure 13: The rotor is made of metal type steel 37-2

Figure 14: Two AMBs, front and rear

6. Results and discussion

Figures 15 and 16 illustrate a test method of the AMB which was carried out in the Laboratories of the Ministry of Science and Technology. All results obtained are shown in two Tables 4 and 5. Table 4 includes three voltages 50, 75, and 100 volts when a DC supply is applied to the windings to know the density of the magnetic field generated at each pole, while Table 5 shows the results for the same test under the excitation of an AC supply.

The overall AMB test rig is shown in Figure 17. Table 6 shows that the operating time of the optimized system model was ten minutes (600 seconds) with the following parameters; speed = 5000 r.p.m., Dia. Yoke =186.92 mm, Z-length (deep of model) = 39.267 mm. All of the results listed in this section are up to the steady-state operation, and all readings reach a steady-state almost continuously. These AMBs reach the steady-state within 120 seconds, after which it is fixed to this state. The table shows that the best value obtained for torque is at an air gap length of about 0.85 mm.

Table 7 shows the amount of flux change with time at No-load for the optimal design of AMB having parameters of an air gap of 0.85 mm, dim. Of the stator of 188.92 mm, Z-length of 39.267 mm, and Ws (ThkYoke) of 14.16 mm. Note that when the rotational speed increases, the flux decreases and settles at 120 sec.

Table 4: The Values of magnetic field under different values of the applied voltage (1Gauss = 10^4 Tesla (T))

	Magnetic Field Density (Tesla)		
Pole No.	***50 V***	***75 V***	***100 V***
Pole. 1	0.021	0.029	0.044
Pole. 2	0.023	0.025	0.042
Pole.3	0.05	0.085	0.09
Pole. 4	0.065	0.073	0.13
Pole. 5	0.052	0.072	0.102
Pole. 6	0.053	0.082	0.1035
Pole. 7	0.062	0.08	0.1037
Pole. 8	0.057	0.081	0.076
Pole. 9	0.043	0.078	0.083
Pole. 10	0.034	0.044	0.066
Pole. 11	0.037	0.05	0.067
Pole. 12	0.035	0.051	0.06

Table 5: The values of magnetic field density with 220V AC supply excitation

Pole No.	**Magnetic Field (T)**
Pole. 1	0.0155
Pole. 2	0.0169
Pole.3	0.0148
Pole. 4	0.0192
Pole. 5	0.0149
Pole. 6	0.0204
Pole. 7	0.0160
Pole. 8	0.0175
Pole. 9	0.0199
Pole. 10	0.0149
Pole. 11	0.0165
Pole. 12	0.0195

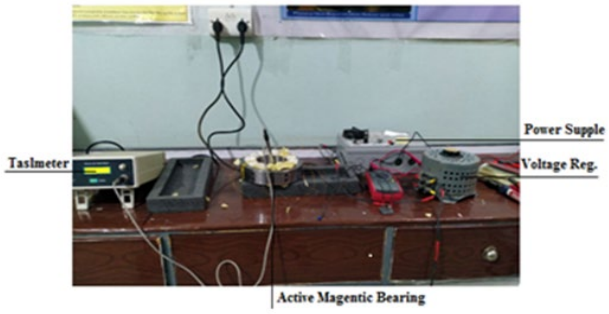

Figure 1: Testing laboratory

Figure 2: The position sensor for testing the magnetic density for each pole

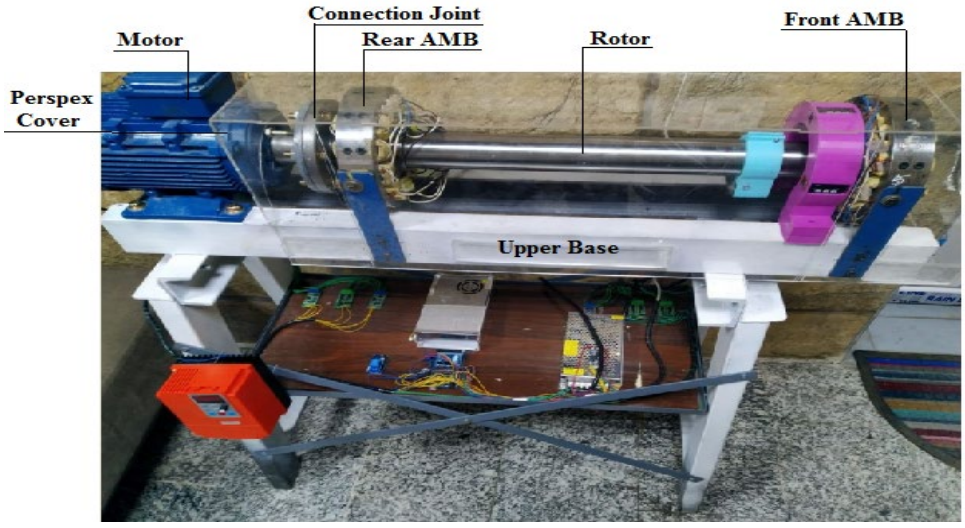

Figure 3: AMB test rig shows the overall system components

Table 6: the torque generated with time under different values of air gap length for The optimal AMB design at No-load

No.	Time (sec.)	Air gap length (at No-load) mm					
		0.85	**0.95**	**1.025**	**1.5**	**2**	**2.5**
		Torque (N.m)					
1	0	0.0000	0.0000	0.0000	0.0000	0.0000	0.0000
2	30	23.001374	17.001374	20.001442	17.208397	11.452281	10.327588
3	60	39.045854	30.045854	37.999930	26.199602	16.447452	13.309355
4	90	72.246590	60.000090	56.802789	39.201234	27.037451	20.011912
5	120	89.000420	85.127852	80.802770	55.201237	39.997451	25.008791
6	150	89.000449	85.127852	80.802754	55.201240	39.997451	25.008790
7	180	89.000477	85. 127852	80.802738	55.201243	39.997451	25.008789
8	210	89.000505	85. 127852	80.802721	55.201245	39.997451	25.008789
9	240	89.046534	85. 127852	80.802705	55.201248	39.997451	25.008788
10	270	89.000562	85. 127852	80.802688	55.201251	39.997451	25.008787
11	300	89.000590	85. 127852	80.802672	55.201254	39.997451	25.008786
12	330	89.000618	85. 127852	80.802656	55.201257	39.997451	25.008785
13	360	89.000647	85. 127852	80.802639	55.201260	39.997451	25.008785
14	390	89.000675	85. 127852	80.802623	55.201262	39.997451	25.008784
15	420	89.000703	85. 127852	80.802506	55.201265	39.997451	25.008783
16	450	89.000732	85. 127852	80.802590	55.201268	39.997451	25.008782
17	480	89.000760	85. 127852	80.802573	55.201271	39.997451	25.008781
18	510	89.000788	85. 127852	80.802557	55.201274	39.997451	25.008781
19	540	89.000817	85. 127852	80.802541	55.201277	39.997451	25.008780
20	570	89.000845	85.127852	80.802524	55.201279	39.997451	25.008779
21	600	89.000873	85.127852	80.802508	55.201282	39.997451	25.008778

Table 7: Flux with time under different values of speed for the optimal AMB design at No-load

No.	Time (sec.)	Speed (at No-load) r.p.m				
		1000	**2000**	**3000**	**4000**	**5000**
				Flux (Wb)		
1	0	0	0	0	0	0
2	30	13.940172	9.025991	8.988677	5.000030	2.030023
3	60	27.198333	23.025768	17.768694	10.925414	5.2215402
4	90	46.246801	40.025969	29.788123	16.882157	12.905469
5	120	71.839865	57.025970	42.928661	35.029014	30.030011
6	150	71.839865	57.025971	42.928661	35.029014	30.030011
7	180	71.839865	57.025972	42.928661	35.029014	30.030011
8	210	71.839865	57.025973	42.928662	35.029014	30.030011
9	240	71.839865	57.025974	42.928662	35.029014	30.030011
10	270	71.839865	57.025974	42.928662	35.029014	30.030011
11	300	71.839865	57.025974	42.928662	35.029014	30.030011
12	330	71.839865	57.025974	42.928662	35.029015	30.030012
13	360	71.839865	57.025974	42.928663	35.029015	30.030012
14	390	71.839865	57.025974	42.928663	35.029015	30.030012
15	420	71.839865	57.025974	42.928663	35.029015	30.030012
16	450	71.839865	57.025974	42.928663	35.029015	30.030012
17	480	71.839865	57.025974	42.928663	35.029015	30.030012
18	510	71.839865	57.025975	42.928663	35.029015	30.030012
19	540	71.839865	57.025975	42.928663	35.029015	30.030012
20	570	71.839865	57.025975	42.928663	35.029015	30.030012
21	600	71.839865	57.025975	42.928664	35.029015	30.030012

7. Conclusions

From the results of the present work, the following conclusions are obtained:

1) The air gap is important in the performance of the AMB. The higher its value, the less is the magnetic force generated in the coils, and consequently, the rotational torque will decrease. As well as if the value of the air gap is small, less than 0.5mm, will lead to friction between the rotor and end of poles. The higher the value of the external load will lead to a decrease in the value of the rotational torque.
2) The goal of the optimal design was achieved in this research by the genetic algorithm method which reduced the number of poles from 16 to 12 and thus the size and mass also decreased while the torque and magnetic flux increased.
3) The complications in the control system will be reduced when they are linked in AMB. The complexities of the control system are inversely proportional to the number of poles.
4) The model covered in this study is made of a material with good engineering and magnetic characteristics steel 37-2.
5) It was noticed that increasing the rotational speed would increase the torque. This is a scientific fact documented in most research, but if the design of the datum is correct in terms of using theoretical equations.
6) The rotational torque value obtained from the rotation of the system was calculated theoretically at the maximum rotational speed where the torque value was 89.000873 N.m without load and 82.292360 N.m. with a load. The values of the (GA) method are considered the best values, as the best values are chosen from among the variables of the system after optimizing them.

Nomenclature

H	intensity of magnetic field
B	density of magnetic flux
P	density of volume charge
D	density of electric charge
Σ	electric conductivity
E	permittivity
M	permeability
μ_0	permeability of free space
J	current density
F	magnetic force
Q	total electric charge
E	electric field
∇	denotes the three-dimensional gradient operator
ε_r	relative permittivity
ε_0	permittivity of free space

Author contribution

All authors contributed equally to this work.

Funding

This research received no specific grant from any funding agency in the public, commercial, or not-for-profit sectors.

Data availability statement

The data that support the findings of this study are available on request from the corresponding author.

Conflicts of interest

The authors declare that there is no conflict of interest.

References

[1] L. V. Rao , S. K. Kakoty, Design of Compact Active Magnetic Bearing, Int. J. App. Sci. Eng. Res., 3 (2014). https://doi.org/10.1109/SCES.2012.6199025

[2] T. J. Yeh, Design, Analysis and Control of a Semi-active Magnetic Bearing System for Rotating Machine Applications, Int. Conf. Info. Con. Aut. Rob., (2015).

[3] G. Martynenko, Resonance Mode Detuning In Rotor Systems Employing Active And Passive Magnetic Bearings With Controlled Stiffness, Int. J. Auto. Mec. Eng. , 13 (2016) 3293 – 3308.

https://doi.org/10.15282/ijame.13.2.2016.2.0274

[4] P. O. Ansah, A. F. Justice, P. K. Agyemang, S. K. Woangbah, Modal Analysis of Rotating Structures with Active Magnetic Bearing, J. Mec. Civil. Eng., 13 (2016) 75-80. https://doi.org/10.9790/1684-1304027580

[5] M. A. Hili, S. Bouaziz, M. Haddar, Stability Analysis and Dynamic Behaviour of A Flexible Asymmetric Rotor Supported By Active Magnetic Bearings, J. Theor. Appl. Mech., 55 (2017) 751-763. https://doi.org/10.15632/jtam-pl.55.3.751

[6] H. Spece, R. Fittro , C. Knospe, Optimization of Axial Magnetic Bearing Actuators for Dynamic Performance, Actuators, 7 (2018) 66. https://doi.org/10.3390/act7040066

[7] S. Ran, Y. Hu , H. Wu, Design, Modeling, And Robust Control Of The Flexible Rotor To Pass The First Bending Critical Speed With Active Magnetic Bearing, Adv. Mech. Eng., 10 (2018).

[8] Z. Zhixian, J. Bolonga, W. Jiayuana, L. Yixina Z. Changshengb, Analysis of Vibration Characteristics of PD Control Active Magnetic Bearing and Cracked Rotor System, Int. J. Eng., 32 (2019).

[9] W. Zhang , H. Zhu, Radial Magnetic Bearings: An Overview, Results. Phys., 7 (2017) 3756–3766. https://doi.org/10.1016/j.rinp.2017.08.043

[10] P.K Agarwal , S. Chand, Fuzzy Logic Control of Three-Pole Active Magnetic Bearing System, Int. Jo. Mod. Ident. Cont., 12 (2011) 395-411 .

[11] W. Zhong, A Review of Active Magnetic Bearings Supported Systems Optimization Design, Int. j. magn. Electromagn., 6 (2020) 2631-5068. http://doi.org/10.35840/2631-5068/6527

[12] E. G. Alcaide, L. P.Acosta , P. K. Kiyohara , R. F. Jardim, Diamagnetic, Paramagnetic, and Ferromagnetic Properties of Ball Milled $Bi_{1.65}$ Pb $_{0.35}Sr_2Ca_2Cu_3O_{10+\delta}$ Powders, J. Nan. Res., 17 (2015) 432.

[13] Z. Zhixian, J. Bolonga, W. Jiayuana, L. Yixina , Z. Changshengb, Analysis of Vibration Characteristics of PD Control Active Magnetic Bearing and Cracked Rotor System, Int. J. Eng., 32 (2019) 596-601.